

Geometric Isotope Effect of Various Intermolecular and Intramolecular C–H···O Hydrogen Bonds, Using the Multicomponent Molecular Orbital Method

Taro Udagawa,[†] Takayoshi Ishimoto,^{*,‡,§} Hiroaki Tokiwa,^{||} Masanori Tachikawa,[†] and Umpei Nagashima^{‡,§}

Quantum Chemistry Division, Graduate School of Science, Yokohama-City University, Seto 22-2, Kanazawa-ku, Yokohama, Kanagawa 236-0027, Japan, Research Institute for Computational Sciences, National Institute of Advanced Industrial Science and Technology, Umezono 1-1-1, Tsukuba, Ibaraki 305-8561, Japan, CREST, Japan Science and Technology Agency, Honcho 4-1-8, Kawaguchi, Saitama 332-0012, Japan, and Department of Chemistry, Faculty of Science, Rikkyo University, Nishi-Ikebukuro 3-34-1, Toshima-ku, Tokyo 171-8501, Japan

Received: March 14, 2006; In Final Form: April 10, 2006

The geometric isotope effect (GIE) of sp- (acetylene–water), sp²- (ethylene–water), and sp³- (methane–water) hybridized intermolecular C–H···O and C–D···O hydrogen bonds has been analyzed at the HF/6-31++G** level by using the multicomponent molecular orbital method, which directly takes account of the quantum effect of proton/deuteron. In the acetylene–water case, the elongation of C–H length due to the formation of the hydrogen bond is found to be greater than that of C–D. In contrast to sp-type, the contraction of C–H length in methane–water is smaller than that of C–D. After the formation of hydrogen bonds, the C–H length itself in all complexes is longer than C–D and the H···O distance is shorter than D···O, similar to the GIE of conventional hydrogen bonds. Furthermore, the exponent (α) value is decreased with the formation of the hydrogen bond, which indicates the stabilization of intermolecular C–H···O hydrogen bonds as well as conventional hydrogen bonds. In addition, the geometric difference induced by the H/D isotope effect of the intramolecular C–H···O hydrogen bond shows the same tendency as that of intermolecular C–H···O. Our study clearly demonstrates that C–H···O hydrogen bonds can be categorized as typical hydrogen bonds from the viewpoint of GIE, irrespective of the hybridizing state of carbon and inter- or intramolecular hydrogen bond.

1. Introduction

Recently, the C–H···O hydrogen bond has received a lot of attention experimentally and theoretically. Although the interaction of C–H···O is weaker than that of typical hydrogen bonds (e.g., O–H···O and N–H···O), C–H···O hydrogen bonds play an important role in the molecular recognition process,¹ biological macromolecules,^{2,3} determination of molecular structure and conformation,^{4–9} and so on.

It is well-known that the bond distance of C–H, in which the proton donor is sp-hybridized, elongates with the formation of the C–H···O hydrogen bond like the typical O–H···O and N–H···O type. On the other hand, in a subset of C–H···O hydrogen bonds in which the proton donor is sp³-hybridized the hydrogen-bonded C–H contracts due to the interaction with a proton acceptor.^{10–12} Since uncharacteristic bond shortening leads the C–H stretching vibration toward a higher frequency, this type of hydrogen bond is called a “blue-shifting hydrogen bond”. This C–H contraction was first reported by Yoshida et al.,¹³ and it sharply contrasts with the X–H (X = O and N) elongation in typical hydrogen bonds.^{14,15} The hybridizing state of carbon and the substituent effect are considered as two factors contributing to these C–H changes.^{16,17}

Many theoretical reports were published to explore the origin of this C–H contraction in C–H···O.^{18–23} Hobza and Havlas^{24,25} concluded that the origin of the blue-shifting hydrogen bond could be explained by charge transfer using natural bond orbital analysis. In the blue-shifting hydrogen bond, the charge transfer from the lone pairs of the proton acceptor atom is mainly directed to the antibonding orbitals in the remote part of the proton donor molecule, while in conventional X–H···O hydrogen bonds, it is mainly directed to the X–H antibonding orbitals of the proton donor molecule. This charge transfer induces the elongation of the covalent bond in the remote atom, structural reorganization, and C–H contraction accordingly. Thus, Hobza and Havlas suggested that blue-shifting hydrogen bonds differ from typical hydrogen bonds. They called the blue-shifting hydrogen bond the “improper hydrogen bond”. In contrast, Scheiner and Kar²⁶ found that the C–H···O hydrogen bonds were like the O–H···O hydrogen bonds regarding geometric behavior and charge distribution. They concluded that there was no fundamental distinction between the blue-shifting hydrogen bonds and typical red-shifting hydrogen bonds. In a recent paper, Li and co-workers¹⁴ found that the blue-shifting hydrogen bond systems did not require either a carbon center or the absence of a lone pair on the proton donor and that the interactions of the blue-shifting hydrogen bond were predominantly electrostatic. According to their analyses, attractive and repulsive interactions exist in all types of hydrogen bonds, only the balance of these interactions is different between the typical and blue-shifting hydrogen bonds. They concluded that the same

* Address correspondence to this author. E-mail: t.ishimoto@aist.go.jp. Phone: +81-298-61-5080 (ext. 55465). Fax: +81-298-51-5426.

[†] Yokohama-City University.

[‡] National Institute of Advanced Industrial Science and Technology.

[§] CREST, Japan Science and Technology Agency.

^{||} Rikkyo University.

interactions underlie both typical and blue-shifting hydrogen bonds. Alabugin and co-workers¹⁵ have also concluded that there was no fundamental difference between the typical and blue-shifting hydrogen bonds. They suggested that the difference between the “improper” and the “proper” hydrogen bond is the strength of hyperconjugative $n(Y) \rightarrow \sigma^*(X-H)$ interaction. If this assumption is fulfilled, a blue-shifting hydrogen bond is possible for N–H and even for O–H bonds.

As mentioned above, much theoretical and experimental research about C–H \cdots O hydrogen bonds is being conducted, but the properties of C–H \cdots O hydrogen bonds have not been identified clearly yet. To our knowledge, no theoretical or experimental studies on the geometric isotope effect (GIE) in C–H \cdots O hydrogen bonds have been reported except in our previous article.²⁷ The bond length (R_{XO}) in the typical X–H(D) \cdots O (e.g., X = O and N) hydrogen bond becomes longer, and the covalent X–H (or X–D) bond length elongates with the formation of the hydrogen bonds. In addition, the X–H length is longer than the corresponding X–D, and the H \cdots O distance accordingly is shorter than the corresponding D \cdots O after formation of the hydrogen bond.²⁸ This GIE is known to be important in determining the physical properties, such as the structural phase transition temperature of hydrogen-bonded dielectric materials²⁹ and the lattice constant of crystals.

To explore the origin and detail of the C–H \cdots O hydrogen bonds, we must clarify the geometric changes induced by the H/D isotope effect. In our previous study, we clarified the GIE in the blue-shifting sp^3 -C–H \cdots O hydrogen bond for the first time. We had already revealed theoretically the geometric and electronic changes in typical O–H \cdots O hydrogen bonds in the water dimer, N–H \cdots O hydrogen bonds in the ammonia–water complex, and C–H \cdots O hydrogen bonds in the methane–water complex by using the multicomponent molecular orbital (MC-MO) method,^{30,31} which directly takes account of the quantum effect of the proton/deuteron as well as the electrons. We have revealed that the C–D length in C–D \cdots O hydrogen bonds became shorter with the formation of a hydrogen bond like the C–H shortening in the C–H \cdots O type bond. In addition, the C–D shortening in the C–D \cdots O hydrogen bond is greater than the C–H shortening in the C–H \cdots O type bond.

In the previous study, we analyzed only the GIE of the blue-shifting intermolecular C–H \cdots O hydrogen bond in the methane–water complex in which carbon is sp^3 -hybridized. For the universal understanding of the C–H \cdots O hydrogen bond, it is necessary to reveal the GIE of both the red-shifting C–H \cdots O hydrogen bond and the intramolecular C–H \cdots O hydrogen bond systematically. A major part of the sp -hybridized intermolecular C–H \cdots O hydrogen bond indicates the red shift of its C–H stretch, and it is known that the geometric changes in the sp^2 -hybridized intermolecular C–H \cdots O hydrogen bond with formation of the hydrogen bond are very small.^{16,17} It is also important to analyze the intramolecular C–H \cdots O hydrogen bond because C–H \cdots O hydrogen bonds exist in various fields as both inter- and intramolecular hydrogen bonds.

In this study, we clarify the GIE of sp -, sp^2 -, and sp^3 -hybridized intermolecular and sp^3 -hybridized intramolecular C–H \cdots O and C–D \cdots O hydrogen bonds to explore the detail of the C–H \cdots O hydrogen bonds.

2. Computational Method

We used the following cluster models for the intermolecular hydrogen bond: acetylene–water ($C_2H_2\cdots H_2O$, AcW), ethylene–water ($C_2H_4\cdots H_2O$, EW), methane–water ($CH_4\cdots H_2O$, MW), and methyleneimine–water ($CH_2NH\cdots H_2O$, MiW) com-

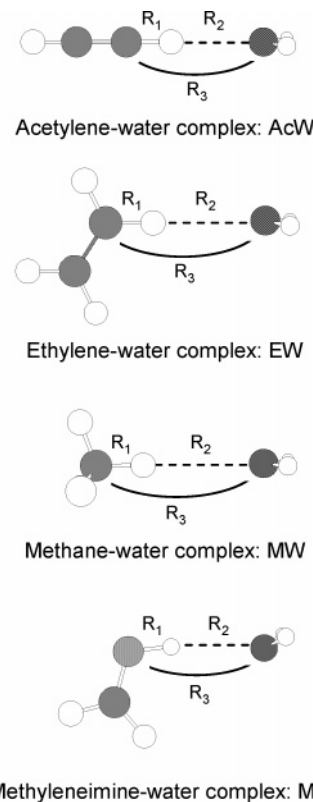


Figure 1. Intermolecular hydrogen-bonded cluster systems.

plexes. We also used three molecules, 1-methoxy-2-(hydroxythio)ethane ($CH_3OCH_2CH_2SOH$, Intra-O–H \cdots O), 1-methoxy-2-(aminothio)ethane ($CH_3OCH_2CH_2SNH_2$, Intra-N–H \cdots O), and 1-methoxy-2-(methylthio)ethane ($CH_3OCH_2CH_2SCH_3$, Intra-C–H \cdots O) as models of intramolecular O–H \cdots O, N–H \cdots O, and C–H \cdots O hydrogen bonds, respectively. The optimized structure and three parameters of each intermolecular cluster model are shown in Figure 1, and the optimized structure and two parameters of each intramolecular model are shown in Figure 2: (a) R_1 , the covalent bond (X–H or X–D, X = O, N, and C) length; (b) R_2 , the H \cdots O (or D \cdots O) distance; and (c) R_3 , the X \cdots O distance. Harada et al.⁶ studied the conformational stabilities of 1-methoxy-2-(methylthio)ethane and relevant intramolecular C–H \cdots O interactions by matrix-isolation infrared spectroscopy and density functional calculations.

To theoretically explore the isotope effect, we used the MC-MO method with 6-31++G** for the electronic basis function. Thresholds for integral evaluation, self-consistent field (SCF) convergence, and root-mean-square displacement of geometry optimization hold very tightly for the discussion of small differences in geometric parameters: 10^{-15} , 10^{-10} , and 4×10^{-6} au, respectively. In this MC-MO calculation, only the hydrogen-bonded proton/deuteron was treated as the quantum wave as well as electrons under the field of nuclear point charges of heavy atoms. The positions of the nuclear point charges were determined by ordinary optimization procedures, using analytical gradients.³² We employed the single s-type ([1s]) Gaussian type function (GTF), $\exp\{-\alpha(r - R)^2\}$, for each protonic and deuteronic basis function, and optimized two variational parameters (α and R), simultaneously. Also, to evaluate the effect of the distribution of the protonic/deuteronic wave function, we employed the single s- and p-type ([1s1p]) GTFs for each protonic and deuteronic basis function, and simultaneously optimized α and R . The centers of electronic GTFs were fixed on each nucleus. All calculations were carried out at the

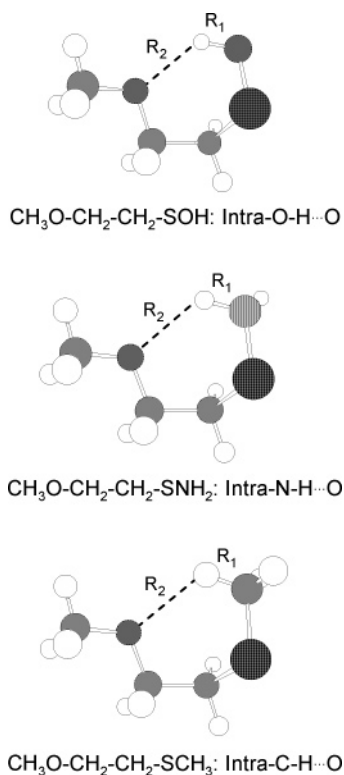


Figure 2. Intramolecular hydrogen-bonded cluster systems.

Hartree–Fock level with the GAUSSIAN 03 program,³³ embedded in the MC-MO method.

The effect of electron correlation is important and cannot be ignored when determining the structures of C–H...O hydrogen bonds because of the dispersion force in the long H...O hydrogen bond distance. In addition, the proton/deuteron–electron correlation signifies the effect of the quantum nature of the proton/deuteron, and it appears only by considering the quantum effect of the proton/deuteron as in our MC-MO calculation. However, Li and co-workers have reported that electron correlation is not a primary cause of this specific C–H contraction.¹⁴ In addition, we have elucidated the calculations at the Hartree–Fock level can be used to evaluate the geometric differences induced by the isotope effect because the effects of electron correlation and proton/deuteron–electron correlation almost canceled each other out with respect to the isotope effect, as shown in the previous paper.²⁷

3. Results and Discussion

3.1. Intermolecular Hydrogen Bonds. *3.1.1. The GIE of AcW, EW, MW, and MiW.* We have calculated the geometric difference induced by the H/D isotope effect of C–H...O and C–D...O hydrogen bonds in the AcW and EW complexes by using the MC-MO method with the [1s] GTF for each protonic

and deuteronic basis function. The optimized parameters of these complexes are shown in Table 1. The definitions of R_1 , R_2 , and R_3 are shown in Figure 1. The notations r_1 and ΔR refer to the C–H (or C–D) length in each monomer and the difference between R_1 and r_1 , respectively.

First, in the sp-hybridized C–H...O hydrogen bond in AcW, the calculated values of $\Delta R(\text{C–H})$ and $\Delta R(\text{C–D})$ were 6.0 and 5.4 mÅ, respectively. These results reproduce the $R_1(\text{C–H})$ elongation and predict the $R_1(\text{C–D})$ elongation with the formation of the C–H(D)...O hydrogen bond. The calculated values of $R_2(\text{H...O})$ and $R_2(\text{D...O})$ were 2.208 and 2.222 Å, respectively. The GIE in AcW shows the same tendency as that of typical O–H...O and N–H...O hydrogen bonds.^{27,28} Second, in the sp²-hybridized C–H...O hydrogen bond in EW, the calculated value of $\Delta R(\text{C–H})$ was 0.2 mÅ. We obtained a tiny bit of the $R_1(\text{C–H})$ elongation with the MC-MO calculation in the present study, even though the conventional MO method obtained a C–H contraction in EW.²⁶ In addition, the geometric changes did not appear in $R_1(\text{C–D})$ with the formation of the hydrogen bond. However, the hydrogen-bonded distance $R_2(\text{H...O})$ (2.539 Å) is shorter than $R_2(\text{D...O})$ (2.554 Å) and $R_1(\text{C–H})$ is longer than $R_1(\text{C–D})$, as with the GIE of the typical hydrogen bonds. On the other hand, in the sp³-hybridized C–H...O hydrogen bond in MW, the calculated values of $\Delta R(\text{C–H})$ and $\Delta R(\text{C–D})$ were –0.5 and –0.6 mÅ, respectively. The results of our calculation show contractions of R_1 in C–H...O and C–D...O hydrogen bonds, as reported in our previous paper.²⁷ The hydrogen-bonded distance $R_2(\text{H...O})$ (2.760 Å) is shorter than $R_2(\text{D...O})$ (2.787 Å), and $R_1(\text{C–H})$ is longer than $R_1(\text{C–D})$, like the typical O–H...O and N–H...O hydrogen bonds. Concerning the geometric changes of ΔR with the formation of the hydrogen bond, although the C–H and C–D elongations in AcW show the same tendency as well as the typical O–H...O and N–H...O hydrogen bonds, the C–H and C–D contractions in MW seem to be different from the changes in typical hydrogen bonds. However, after the formation of the hydrogen bond, $R_1(\text{C–H})$ is longer than $R_1(\text{C–D})$, and $R_2(\text{H...O})$ is shorter than $R_2(\text{D...O})$ in all complexes.

3.1.2. The Calculated α Values and Electronic Charge Densities. We next show the optimized α value in Table 2. α_{mono} means the optimized α value in [1s] GTF of the proton/deuteron in each monomer. The notation of $\Delta\alpha$ refers to the difference between the optimized α value in complex and α_{mono} . In all types of complexes, negative $\Delta\alpha$ values mean the delocalization of proton/deuteron with the formation of a hydrogen bond. The $\Delta\alpha$ value of proton (deuteron) in AcW, EW, and MW was –0.46 (–0.62), –0.22 (–0.31), and –0.20 (–0.23), respectively. The difference between the wave function of a proton and that of a deuteron reflects the geometric difference induced by the H/D isotope effect because of the anharmonicity of the potential. The wave function of the deuteron became more delocalized with the formation of hydrogen bonds in all types of complexes, because the absolute values of $\Delta\alpha$ in deuterons

TABLE 1: Optimized Geometric Parameters of C–H(D)...O in Acetylene–Water, Ethylene–Water, Methane–Water, and Methyleneimine–Water Complexes at the HF/6-31++G Level, Using the MC-MO**

	AcW		EW		MW		MiW	
	H	D	H	D	H	D	H	D
r_1^a [Å]	1.0785	1.0722	1.0979	1.0915	1.1059	1.0993	1.0268	1.0204
R_1 [Å]	1.0845	1.0776	1.0981	1.0915	1.1054	1.0987	1.0280	1.0213
ΔR^b [mÅ]	6.0	5.4	0.2	0.0	–0.5	–0.6	1.2	0.9
R_2 [Å]	2.208	2.222	2.539	2.554	2.760	2.787	2.223	2.239
R_3 [Å]	3.293	3.300	3.636	3.645	3.866	3.885	3.245	3.250

^a r_1 indicates the C–H (or N–H) length in each monomer. ^b ΔR is defined as $R_1 - r_1$.

TABLE 2: Optimized α Values of Proton and Deuteron and Electronic Charge Densities Calculated by Using Mulliken Population Analysis in AcW, EW, MW, and MiW

	AcW		EW		MW		MiW	
	H	D	H	D	H	D	H	D
α_{mono}	23.98	35.35	24.79	36.50	24.51	36.15	24.37	35.95
α	23.52	34.73	24.57	36.19	24.71	36.38	24.70	36.40
$\Delta\alpha^a$	-0.46	-0.62	-0.22	-0.31	-0.20	-0.23	-0.33	-0.45
X_{mono}^b	-0.208	-0.203	-0.226	-0.226	-0.481	-0.474	-0.441	-0.434
$H_{\text{others mono}}^c$			-0.882	-0.884	-0.883	-0.884		
$H(\text{D})_{\text{mono}}^d$	-0.777	-0.785	-0.875	-0.878	-0.870	-0.874	-0.720	-0.726
X^b	-0.236	-0.221	-0.227	-0.226	-0.450	-0.447	-0.480	-0.473
O	-0.745	-0.744	-0.727	-0.727	-0.717	-0.717	-0.754	-0.754
H_{others}^c			-0.883	-0.885	-0.891	-0.891		
$H(\text{D})^d$	-0.723	-0.726	-0.930	-0.929	-0.894	-0.893	-0.669	-0.675
$\Delta H(\text{D})^e$	0.054	0.059	-0.055	-0.051	-0.024	-0.019	0.051	0.051

^a $\Delta\alpha$ is defined as $\alpha - \alpha_{\text{mono}}$. ^b X is a center atom in proton donor. ^c H_{others} are nonhydrogen-bonded protons in the proton donor. ^d $H(\text{D})$ is the hydrogen-bonded proton in the proton donor that is treated as the quantum wave. ^e $\Delta H(\text{D})$ is defined as $H(\text{D}) - H(\text{D})_{\text{mono}}$.

were always larger than those in protons. The electrostatic interaction in EW and MW is weak because the wave function of proton/deuteron delocalizes only a little with the formation of the hydrogen bonds. However, these results of $\Delta\alpha$ values represent the same electrostatic interaction underlying even blue-shifting C–H \cdots O hydrogen bonds.

Table 2 also lists the electronic charge densities calculated by using Mulliken population analysis³⁴ of AcW, EW, and MW. The notation $\Delta H(\text{D})$ refers to the difference between $H(\text{D})$ in complex and $H(\text{D})_{\text{mono}}$. We can find two patterns in these results. First, the electronic charge density around the hydrogen-bonded proton/deuteron became electropositive with the formation of the hydrogen bond like the typical O–H \cdots O and N–H \cdots O hydrogen bonds. This pattern can be found in AcW (0.054/0.059). Second, the electronic charge density around the hydrogen-bonded proton/deuteron became electronegative with the formation of the hydrogen bond. This pattern can be found in EW (-0.055/-0.051) and MW (-0.024/-0.019). The changes of the electronic charge density induced by the H/D isotope effect in EW and MW differ from that of typical hydrogen bonds.

In the EW, although the geometric change seems to follow the same tendency as that of the typical hydrogen bonds, the change of electronic charge density is similar to the case of MW. To explore this singular result in detail, we have calculated AcW, EW, and MW clusters with [1s1p] GTFs for the protonic/deuteron wave function. The calculated $\alpha(\text{X})$ ($\text{X} = \text{s}$ - and p -type GTFs) values and electronic charge densities with the [1s1p] GTFs for the protonic and deuteron wave function of the AcW, EW, and MW are shown in Table 3. The geometric changes, α value, and electronic charge densities are not so different from the results using only [1s] GTF for the wave function of the proton/deuteron, though elongation appeared in $R_1(\text{C}-\text{D})$ in EW. The geometric changes in EW are like those of typical hydrogen bonds, but the changes of electronic charge densities show the same tendency in the case of blue-shifting hydrogen bonds.

We show the linear combination of atomic orbital (LCAO) coefficients of the wave functions for proton/deuteron in Table 4, where we set hydrogen-bonded H \cdots O (or D \cdots O) along the X axis. The coefficients of 1s, p_x , p_y , and p_z of GTFs of proton/deuteron in EW were 0.99018/0.98994, 0.13966/0.14137, -0.00609/-0.00630, and 0.00000/0.00000, respectively. In addition those values in MW were 0.98888/0.98882, 0.14874/0.14911, -0.00054/-0.00054, and -0.00001/-0.00001, respectively. Because of the hydrogen bond, the coefficient of p_x

TABLE 3: Optimized Geometric Parameters, α Values, and Electronic Charge Densities in AcW, EW, and MW Calculated by Using Both s- and p-Type GTFs as the Wave Function of Proton/Deuteron

	AcW		EW		MW	
	H	D	H	D	H	D
r_1 [\AA]	1.0590	1.0562	1.0821	1.0784	1.0892	1.0855
R_1 [\AA]	1.0656	1.0621	1.0825	1.0785	1.0888	1.0850
ΔR [$\text{m}\text{\AA}$]	6.6	5.9	0.4	0.1	-0.4	-0.5
R_2 [\AA]	2.227	2.237	2.555	2.569	2.782	2.807
R_3 [\AA]	3.293	3.299	3.638	3.647	3.871	3.892
$\alpha(\text{s})_{\text{mono}}^a$	23.98	35.35	24.79	36.50	24.71	36.38
$\alpha(\text{s})$	23.52	34.73	24.57	36.19	24.51	36.15
$\Delta\alpha(\text{s})$	-0.46	-0.62	-0.22	-0.31	-0.20	-0.23
$\alpha(\text{p})_{\text{mono}}^a$	22.91	34.18	23.33	34.89	23.42	34.96
$\alpha(\text{p})$	22.22	33.29	22.96	34.43	23.17	34.64
$\Delta\alpha(\text{p})$	-0.69	-0.89	-0.37	-0.46	-0.25	-0.32
C_{mono}	-0.196	-0.194	-0.215	-0.217	-0.469	-0.465
$H_{\text{others mono}}$			-0.882	-0.883	-0.883	-0.884
$H(\text{D})_{\text{mono}}$	-0.796	-0.801	-0.887	-0.889	-0.881	-0.884
C	-0.224	-0.212	-0.216	-0.217	-0.440	-0.440
O	-0.744	-0.744	-0.727	-0.728	-0.717	-0.717
H_{others}			-0.882	-0.885	-0.891	-0.892
$H(\text{D})$	-0.737	-0.738	-0.940	-0.937	-0.902	-0.900
$\Delta H(\text{D})$	0.060	0.063	-0.053	-0.048	-0.021	-0.016

^a $\alpha(\text{s})$ and $\alpha(\text{p})$ mean the α value of s and p type GTF, respectively.

TABLE 4: LCAO Coefficient Values of the Wave Function of Proton/Deuteron in AcW, EW, and MW

	AcW		EW		MW	
	H	D	H	D	H	D
1s	0.98638	0.98641	0.99018	0.98994	0.98888	0.98882
p_x	-0.16448	-0.16430	0.13966	0.14137	0.14874	0.14911
p_y	0.00000	0.00000	-0.00609	-0.00630	-0.00054	-0.00054
p_z	0.00000	0.00000	0.00000	0.00000	-0.00001	-0.00001

is relatively large. The elongation of $R_1(\text{C}-\text{D})$ appears by using [1s1p] GTFs for the wave function of the proton/deuteron of the EW. However, the tendency of GIE for EW is the same as the results obtained by using only [1s] GTF. This result demonstrates that [1s] GTF is usable for qualitative analysis of GIE.

3.1.3. Classification of Hydrogen Bonds Based on GIE. Figure 3 shows the relationship between ΔR and the number of electrons around the central atom in the proton donor molecule. This figure shows that the values of R^2 were 0.9983 and 0.9987

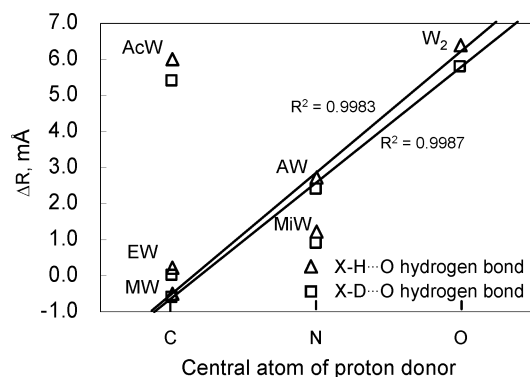


Figure 3. Relationship between ΔR and the number of electrons around the central atom in the proton donor molecule. For W_2 and AW see ref 27.

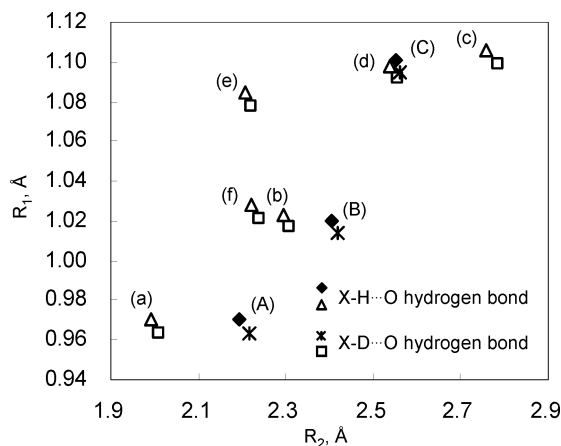


Figure 4. Relationship between R_1 and R_2 . (Lower-case letters mean intermolecular hydrogen bond: (a) W_2 , (b) AW, (c) MW, (d) EW, (e) AcW, and (f) MiW. Upper-case letters mean intramolecular hydrogen bond: (A) Intra-O-H...O, (B) Intra-N-H...O, and (C) Intra-C-H...O.)

for X-H...O and X-D...O hydrogen bond systems, respectively. The results of water dimer (W_2), ammonia-water complex (AW), and MW show an excellent linearity. This means that the MW is not an improper hydrogen bond concerning the geometric difference with the formation of a hydrogen bond. The optimized value ΔR of AcW is almost the same as that of W_2 , and the ΔR of EW tilts toward that of AW. Furthermore, Figure 4 shows the relationship between R_1 and R_2 in each complex. The results of W_2 , AW, and MW show a very good linearity. The difference between these hydrogen-bonded clusters is the number of lone pairs in the proton donor's central atom. This relationship strongly suggests that the same principle for geometric changes underlies the MW, which is a blue-shifting intermolecular C-H...O bond, as well as typical O-H...O and N-H...O intermolecular hydrogen bonds. The results of AcW, EW, and MW also show an excellent linearity. The difference between these hydrogen-bonded clusters is the number of π -bonds. This relationship means the difference in the hybridizing state of carbon does not affect the C-H(D) bond length, but strongly affects ΔR .

To elucidate the effect of lone-pair and π -electron for the hydrogen-bonded system, we have calculated MiW, which has both a lone-pair and a π -bond, at the same level. The optimized structure and parameters of MiW are also shown in Figure 1 and Table 1. The calculated values of $\Delta R(N-H(D))$ and $R_2(H(D)\cdots O)$ were 1.2 mÅ (0.9 mÅ) and 2.223 Å (2.239 Å), respectively. The GIE of MiW shows the same tendency as that

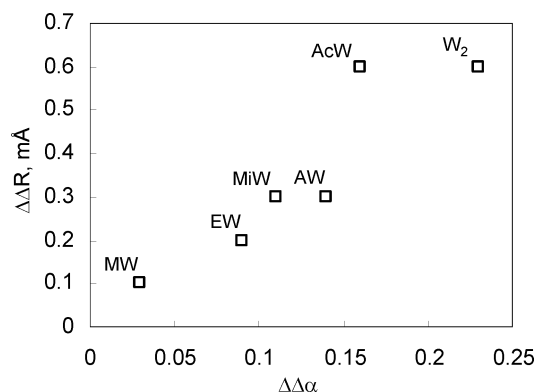


Figure 5. Relationship between $\Delta\Delta R (= \Delta R(H) - \Delta R(D))$ and $\Delta\Delta\alpha (= \Delta\alpha(H) - \Delta\alpha(D))$.

of typical hydrogen bonds, which we show in Figures 3 and 4. The result of MiW locates at a reasonable position, since R_1 of MiW is almost the same as that of AW. Also, because of presence of a π -bond, ΔR and R_2 of MiW are different from those of AW, as well as the case of AcW, EW, and MW systems. ΔR and R_2 are smaller and shorter than those of AW, respectively. Here, we define the $\Delta\Delta R$ as $\Delta R(H) - \Delta R(D)$, which indicates the GIE around the X-H bond, and $\Delta\Delta\alpha$ as $\Delta\alpha(H) - \Delta\alpha(D)$. We find that $\Delta\Delta R$ correlates with $\Delta\Delta\alpha$, irrespective of the hybridizing state of the center atom and species of the center atom (Figure 5). In the MC-MO calculation, the difference of quantum property between proton and deuteron is directly reflected in the geometry, and it appears as the α value in the results. So, the change in the α value with the formation of the hydrogen bond ($\Delta\alpha$) correlates with the change of R_1 (ΔR). Therefore, the $\Delta\Delta R$ with $\Delta\Delta\alpha$ shows a good correlation because the GIE of the C-H...O hydrogen bond is mainly induced by the difference of the quantum property of proton/deuteron, as well as the conventional O-H...O and N-H...O hydrogen bonds.

Although MW is a blue-shifting intermolecular hydrogen bond and the results of EW are a bit curious, all the hydrogen-bonded systems studied here could be categorized from GIE as the same hydrogen bond.

3.2. Intramolecular Hydrogen Bonds. *3.2.1. The GIE of Intra-O-H...O, Intra-N-H...O, and Intra-C-H...O.* To elucidate all the properties of the C-H...O hydrogen bond, we have analyzed the intramolecular hydrogen bonds. We have calculated the geometric difference induced by the H/D isotope effect of intramolecular hydrogen bonds in Intra-O-H...O, Intra-N-H...O, and Intra-C-H...O by using the MC-MO method. The optimized parameters of these complexes are shown in Table 5. We used linear chain molecules as the reference structure for the evaluation of geometric change with the formation of the intramolecular hydrogen bonds. We have calculated these molecules by using the single [1s] GTF for proton and deuteron.

First, in the O-H...O hydrogen bond in Intra-O-H...O, the calculated values of ΔR for O-H...O and O-D...O were 3.2 and 2.9 mÅ, respectively. $R_1(O-H)$ and $R_1(O-D)$ elongated with the formation of the hydrogen bond like the elongation with the intermolecular O-H...O hydrogen bond. Furthermore, $R_1(O-H)$ is longer than $R_1(O-D)$, and $R_2(H\cdots O)$ is shorter than $R_2(D\cdots O)$. These structural profiles are the same as the intermolecular O-H...O hydrogen bond. Second, in the N-H...O hydrogen bond in Intra-N-H...O, $R_1(N-H)$ and $R_1(N-D)$ elongated with the formation of the hydrogen bond, and the hydrogen-bonded structure exhibits the same tendency

TABLE 5: Optimized Geometric Parameters, α Values, and Electronic Charge Densities in Intra-O-H \cdots O, Intra-N-H \cdots O, and Intra-C-H \cdots O

	Intra-O-H \cdots O		Intra-N-H \cdots O		Intra-C-H \cdots O	
	H	D	H	D	H	D
r_1 [Å]	0.9670	0.9605	1.0188	1.0128	1.1045	1.0979
R_1 [Å]	0.9702	0.9634	1.0202	1.0137	1.1010	1.0944
ΔR [mÅ]	3.2	2.9	1.4	0.9	-3.5	-3.5
R_2 [Å]	2.192	2.216	2.406	2.417	2.551	2.561
α_{mono}	23.75	35.06	24.45	36.04	24.65	36.32
α	23.51	34.76	24.28	35.81	24.68	36.35
$\Delta\alpha$	-0.24	-0.30	-0.17	-0.23	0.03	0.03
X_{mono}	-0.650	-0.645	-0.768	-0.761	-0.377	-0.377
$H_{\text{others mono}}$			0.677	-0.678	-0.860	0.861
$H(D)_{\text{mono}}$	-0.586	-0.594	-0.657	-0.664	-0.861	-0.863
X	-0.629	-0.620	-0.753	-0.747	-0.442	-0.441
O	-0.507	-0.505	-0.475	-0.474	-0.442	-0.442
H_{others}			-0.680	-0.680	-0.869	-0.870
$H(D)$	-0.545	-0.554	-0.649	-0.654	-0.842	-0.845
$\Delta H(D)$	0.041	0.040	0.008	0.010	0.019	0.018

as the intermolecular N-H \cdots O hydrogen bond. Finally, in the C-H \cdots O hydrogen bond in Intra-C-H \cdots O, the calculated value of ΔR was -3.5 mÅ for C-H \cdots O and -3.5 mÅ for C-D \cdots O. $R_1(\text{C-H})$ and $R_1(\text{C-D})$ contracted with formation of the hydrogen bonds such as for the intermolecular C-H \cdots O hydrogen bond. In addition the hydrogen-bonded structure exhibits the same tendency as was observed with the formation of the intermolecular C-H \cdots O hydrogen bond, $R_1(\text{C-H})$ is longer than $R_1(\text{C-D})$ and $R_2(\text{H}\cdots\text{O})$ is shorter than $R_2(\text{D}\cdots\text{O})$, respectively. In all types of intramolecular hydrogen bonds, however, the value of ΔR is smaller than that of intermolecular hydrogen bonds. Because of the lower structural flexibility, the hydrogen-bonded distance R_2 is shorter than each intermolecular hydrogen bond. This structural distinction strengthens the repulsive interaction. In Figure 4, we can see that each intramolecular hydrogen bond is shifted in R_2 , at a constant R_1 from each intermolecular hydrogen bond; this divergence is also caused by structural flexibility. However, in all types of intramolecular hydrogen bonds, $R_1(\text{X-H})$ is longer than $R_1(\text{X-D})$ ($X = \text{O}, \text{N}, \text{and C}$), and $R_2(\text{H}\cdots\text{O})$ is shorter than $R_2(\text{D}\cdots\text{O})$. This relationship is the same as observed with intermolecular hydrogen bonds.

Thus, concerning the geometric changes and hydrogen-bonded structures, all intramolecular hydrogen bonds exhibit the same tendency as each intermolecular hydrogen bond.

3.2.2. The Calculated α Values and Electronic Charge Densities. We show the optimized α value in Table 5. The values of $\Delta\alpha$ in proton (deuteron) in Intra-O-H \cdots O, Intra-N-H \cdots O, and Intra-C-H \cdots O were -0.24 (-0.30), -0.17 (-0.23), and 0.03 (0.03), respectively. The $\Delta\alpha$ in Intra-C-H \cdots O is positive, but it is very small. This change of $\Delta\alpha$ is caused by the slight difference in the environment around the proton/deuteron due to use of a linear chain molecule as the reference structure. Table 5 also lists the electronic charge densities using Mulliken population analysis of Intra-O-H \cdots O, Intra-N-H \cdots O, and Intra-C-H \cdots O. The changes of charge density on the proton (deuteron) in Intra-O-H \cdots O, Intra-N-H \cdots O, and Intra-C-H \cdots O were 0.041 (0.040), 0.008 (0.010), and 0.019 (0.018), respectively. The change of Intra-C-H \cdots O indicates a different pattern from intermolecular sp³-C-H \cdots O hydrogen bonds, although those of Intra-O-H \cdots O and Intra-N-H \cdots O indicate the same pattern as intermolecular O-H \cdots O and N-H \cdots O hydrogen bonds. In addition, the lengths of C-H and C-D contract, like the intermolecular

sp³-C-H \cdots O hydrogen bonds do, by forming the intramolecular sp³-C-H \cdots O hydrogen bond; the change of electronic charge on proton/deuteron indicates the same pattern as typical O-H \cdots O and N-H \cdots O hydrogen bonds. This phenomenon should be investigated with a more accurate method that takes many body effects into account.

4. Conclusion

We have analyzed the GIE of sp-, sp²-, and sp³-hybridized C-H \cdots O and C-D \cdots O hydrogen bonds and intramolecular hydrogen bonds by using the MC-MO method, which directly takes into account the quantum effect of proton/deuteron as well as electrons.

The geometric changes in AcW are similar in effect to those of O-H \cdots O and N-H \cdots O hydrogen bonds. In EW, there are no drastic geometric changes with the formation of the hydrogen bonds. The contraction of the C-H (and C-D) length of MW sharply contrasts with AcW as we have already reported. However, after the formation of hydrogen bonds, $R_1(\text{C-H})$ is longer than $R_1(\text{C-D})$ and $R_2(\text{H}\cdots\text{O})$ is shorter than $R_2(\text{D}\cdots\text{O})$ in all complexes, irrespective of the elongation or contraction of $R_1(\text{C-H})$ and $R_1(\text{C-D})$ with the formation of the hydrogen bond, the hybridization of the central atom, and inter- or intramolecular hydrogen bonds. The α values of proton and deuteron became small with the formation of the hydrogen bond. The difference of distribution between proton and deuteron directly reflects the geometries. We clearly demonstrate that the blue-shifting C-H \cdots O hydrogen bond has the same GIE properties as well as the typical O-H \cdots O and N-H \cdots O hydrogen bonds, because the relationship between the $\Delta\Delta R$ and $\Delta\Delta\alpha$ shows good linearity.

Our study reveals that the C-H \cdots O hydrogen bonds are not specific and improper hydrogen bonds with regard to GIE. GIE calculations that consider the quantum nature of protons/deuterons clearly show that the C-H \cdots O hydrogen bonds can be categorized as typical hydrogen bonds.

Acknowledgment. This work was supported by the research project "Development of MO calculation system for large molecule on Grid", CREST, Japan Science and Technology Agency.

References and Notes

- (1) Sarkhel, S.; Desiraju G. R. *Proteins* **2004**, *54*, 247-259.
- (2) Wahl, M. C.; Sundaralingam, M. *Trends Biochem. Sci.* **1997**, *22*, 97-102.
- (3) Jiang, L.; Lai, L. *J. Biol. Chem.* **2002**, *277*, 37732-37740.
- (4) Yoshida, H.; Kaneko, I.; Matsuura, H.; Ogawa, Y.; Tasumi, M. *Chem. Phys. Lett.* **1992**, *196*, 601-606.
- (5) Tsuzuki, S.; Uchimaru, T.; Tanabe, K.; Hirano, T. *J. Phys. Chem.* **1993**, *97*, 1346-1350.
- (6) Harada, T.; Yoshida, H.; Ohno, K.; Matsuura, H. *Chem. Phys. Lett.* **2002**, *362*, 453-460.
- (7) Lo Presti, L.; Soave, R.; Destro, R. *J. Phys. Chem. B* **2006**, *110*, 6405-6414.
- (8) Dzierżawska-Majewska, A.; Obniska, J.; Karolak-Wojciechowska, J. *J. Mol. Struct.* **2006**, *783*, 66-72.
- (9) Torres, H.; Insuasty, B.; Cobo, J.; Low, J. N.; Glidewell, C. *Acta Crystallogr., Sect. C* **2005**, *61*, o404-o407.
- (10) Hobza, P.; Havlas, Z. *Chem. Phys. Lett.* **1999**, *303*, 447-452.
- (11) Harada, T.; Yoshida, H.; Ohno, K.; Matsuura, H.; Zhang, J.; Iwaoka, M.; Tomoda, S. *J. Phys. Chem. A* **2001**, *105*, 4517-4523.
- (12) Matsuura, H.; Yoshida, H.; Hieda, M.; Yamanaka, S.; Harada, T.; Shin-ya, K.; Ohno, K. *J. Am. Chem. Soc.* **2003**, *125*, 13910-13911.
- (13) Yoshida, H.; Harada, T.; Murase, T.; Ohno, K.; Matsuura, H. *J. Phys. Chem. A* **1997**, *101*, 1731-1737.
- (14) Li, X.; Liu, L.; Schlegel, H. B. *J. Am. Chem. Soc.* **2002**, *124*, 9639-9647.
- (15) Alabugin, I. V.; Manoharan, M.; Peabody, S.; Weinhold, F. *J. Am. Chem. Soc.* **2003**, *125*, 5973-5987.

- (16) Hartmann, M.; Wetmore, S. D.; Radom, L. *J. Phys. Chem. A* **2001**, *105*, 4470–4479.
- (17) Scheiner, S.; Grabowski, S. J.; Kar, T. *J. Phys. Chem. A* **2001**, *105*, 10607–10612.
- (18) Hermansson, K. *J. Phys. Chem. A* **2002**, *106*, 4695–4702.
- (19) van der Veken, B. J.; Herrebout, W. A.; Szostak, R.; Shchepkin, D. N.; Havlas, Z.; Hobza, P. *J. Am. Chem. Soc.* **2001**, *123*, 12290–12293.
- (20) Qian, W.; Krimm, S. *J. Phys. Chem. A* **2002**, *106*, 6628–6636.
- (21) Gu, Y.; Kar, T.; Scheiner, S. *J. Am. Chem. Soc.* **1999**, *121*, 9411–9422.
- (22) Masunov, A.; Dannenberg, J. J.; Contreras, R. H. *J. Phys. Chem. A* **2001**, *105*, 4737–4740.
- (23) Dalanoye, S. N.; Herrebout, W. A.; van der Veken, B. J. *J. Am. Chem. Soc.* **2002**, *124*, 7490–7498.
- (24) Hobza, P.; Havlas, Z. *Chem. Rev.* **2000**, *100*, 4253–4264.
- (25) Hobza, P.; Havlas, Z. *Theor. Chem. Acc.* **2002**, *108*, 325–334.
- (26) Scheiner, S.; Kar, T. *J. Phys. Chem. A* **2002**, *106*, 1784–1789.
- (27) Udagawa, T.; Ishimoto, T.; Tokiwa, H.; Tachikawa, M.; Nagashima, U. *Chem. Phys. Lett.* **2004**, *389*, 236–240.
- (28) Dalal, N.; Klymchyov, A.; Bussmann-Holdem, A. *Phys. Rev. Lett.* **1998**, *81*, 5924–5927.
- (29) Tachikawa, M.; Ishimoto, T.; Tokiwa, H.; Kasatani, H.; Deguchi, K. *Ferroelectrics* **2002**, *268*, 3–9.
- (30) Tachikawa, M.; Mori, K.; Suzuki, K.; Iguchi, K. *Int. J. Quantm Chem.* **1998**, *70*, 491–501.
- (31) Tachikawa, M.; Mori, K.; Nakai, H.; Iguchi, K. *Chem. Phys. Lett.* **1998**, *290*, 437–442.
- (32) Pulay, P. In *Application in Electronic Structure Theory*; Schaefer, H. F., Ed.; Plenum Press: New York, 1977.
- (33) Frisch, M. J.; Trucks, G. W.; Schlegel, H. B.; Scuseria, G. E.; Robb, M. A.; Cheeseman, J. R.; Montgomery, J. A., Jr.; Vreven, T.; Kudin, K. N.; Burant, J. C.; Millam, J. M.; Iyengar, S. S.; Tomasi, J.; Barone, V.; Mennucci, B.; Cossi, M.; Scalmani, G.; Rega, N.; Petersson, G. A.; Nakatsuji, H.; Hada, M.; Ehara, M.; Toyota, K.; Fukuda, R.; Hasegawa, J.; Ishida, M.; Nakajima, T.; Honda, Y.; Kitao, O.; Nakai, H.; Klene, M.; Li, X.; Knox, J. E.; Hratchian, H. P.; Cross, J. B.; Adamo, C.; Jaramillo, J.; Gomperts, R.; Stratmann, R. E.; Yazyev, O.; Austin, A. J.; Cammi, R.; Pomelli, C.; Ochterski, J. W.; Ayala, P. Y.; Morokuma, K.; Voth, G. A.; Salvador, P.; Dannenberg, J. J.; Zakrzewski, V. G.; Dapprich, S.; Daniels, A. D.; Strain, M. C.; Farkas, O.; Malick, D. K.; Rabuck, A. D.; Raghavachari, K.; Foresman, J. B.; Ortiz, J. V.; Cui, Q.; Baboul, A. G.; Clifford, S.; Cioslowski, J.; Stefanov, B. B.; Liu, G.; Liashenko, A.; Piskorz, P.; Komaromi, I.; Martin, R. L.; Fox, D. J.; Keith, T.; Al-Laham, M. A.; Peng, C. Y.; Nanayakkara, A.; Challacombe, M.; Gill, P. M. W.; Johnson, B.; Chen, W.; Wong, M. W.; Gonzalez, C.; Pople, J. A. *Gaussian 03*, Revision B.05; Gaussian, Inc.: Pittsburgh, PA, 2003.
- (34) Mulliken, R. S. *J. Chem. Phys.* **1955**, *23*, 1833–1840.